Reconstructing Radiosity by Scattered Data Interpolation

André Hinkenjann, Georg Pietrek
Universität Dortmund
Informatik LS VII
D-44221 Dortmund
Germany

ABSTRACT

We discuss interpolation methods for the reconstruction of the radiosity function across a patch. Two groups of methods are compared: One group based on regular grids and one based on hierarchical subdivisions. We handle points on hierarchical subdivisions as scattered data points which opens the field of scattered data interpolation. These different methods were implemented and characteristic images that show the (dis)advantages are discussed and compared. Additionally, we calculated errors in standard error measures. It shows that some scattered data interpolation methods produce acceptable images.

Keywords: Radiosity reconstruction, interpolation, scattered data.

1 Introduction

The goal of image synthesis is to produce realistic looking pictures of synthetic scenes. Several methods have been proposed, like raytracing [Whi80] or radiosity [GTGB84]. We will restrict ourselves to the radiosity method with constant basis functions across the subdivision-patches. The problem that arises from this type of functions is that the resulting radiosity is constant across a patch. This results in facetted surfaces in the final pictures. To solve this problem, interpolation across the patches is used.

In the case of regular subdivisions (eg a grid) the radiosity values at the vertices of the subdivison cells (eg quadrilaterals) are used to determine the values of the radiosity function inside a cell. This can be done by bilinear or bicubic spline interpolation, just to name some of the methods. All of these methods have advantages and disadvantages as discussed below. Typically, pictures calculated from the radiosity method are rendered on high-end graphics workstations. As of today, bilinear interpolation across the subdivision-patches of the polygons is implemented in hardware.

In the case of hierarchical subdivisions (eg a quadtree) interpolation directly from the vertices produces visual artefacts, like that from T-vertices. Therefore, hierarchical subdivisions have to be treated further. A common approach to solve the problems is to triangulate the subdivision and to interpolate across the newly generated triangles using some of the above mentioned interpolation methods (compare [CW93], pages 147-149). This has the disadvantage of producing even more patches and taking over the disadvantages of the traditional interpolation methods.

One approach for continuous radiosity reconstruction uses Clough-Tocher elements constructed from cubic triangular Bézier patches [SLD92]. This results in a C^1-continuous reconstruction. Discontinuities are taken into account by relaxing continuity conditions of the Clough-Tocher construction. Bastos et al. use bicubic Hermite interpolation for regular [BdSF93] or quadtree [BGZ96] subdivisions. Derivatives needed for the Hermite interpolation are estimated from the radiosity samples. Here discontinuities can be incorporated by duplicating vertices along discontinuity edges. While these approaches have advantages, most radiosity programs do not implement discontinuity meshing [LTG92] because it requires non trivial algorithms and increases computing time.

We have concentrated on reconstruction methods for radiosity solutions without discontinuity meshing. Several interpolation methods for regular and hierarchical patch subdivisions were implemented and compared.

We present an approach that treats radiosity values from hierarchical subdivisions as scattered data. This approach has been identified as "a largely untapped source of potentially useful techniques for radiosity and image synthesis" [CW93]. Although scattered data interpolation methods are well known in other application fields our approach is to our knowledge the first application of these methods for radiosity reconstruction.

This introduces methods of the field of scattered data interpolation where functions $f : \mathbb{R}^d \rightarrow \mathbb{R}$ are reconstructed from function values of arbitrary data points. Several interpolation methods exist which have their specific application fields [Alf89, Nie93]. We will concentrate on *distance weighted interpolation*, *Hardy's Multiquadrics*, and *natural neighbour interpolation*.

2 Discussion of interpolation methods

Let us assume we have a point $\mathbf{q} = (x_d, y_d)$ on a patch for which we want to determine the radiosity value $B(\mathbf{q})$. Interpolation methods will return an approximate $\tilde{B}(\mathbf{q})$ calculated from the set of known radiosity values $B(\mathbf{p}_i), i = 1 \ldots n$.

We have implemented two groups of interpolation methods: one for regular patch subdivisions and the other for adaptive, hierarchical subdivisions. The latter can also be used for regular patch subdivisions but not vice versa.

To evaluate the quality of the different methods and compare them, images of several sample scenes were generated using the different methods. Due to size restrictions only results from one scene are presented. Fig. 2 shows a reference solution for this sample scene that was calculated by a progressive radiosity program using a regular 400 by 400 patch subdivision. We are interested in the radiosity of the ground patch. The scene is lit by a rectangular light source above the ground patch. Shadows are thrown by two perpendicular patches standing on the ground. The left image in Fig. 2 shows a view into this scene, the middle image is an enlarged portion of the left image, showing an interesting region of the ground, and the right image shows the radiosity distribution over the ground patch. Each row of the Figures 3 and 4 illustrates the result of a particular interpolation method. The left and middle images show the views known from the reference solution, the right image shows the difference between the interpolated radiosity and the reference solution, scaled by a factor of two. Medium grey pixels represent zero difference, bright pixels indicate positive difference, dark pixels show negative difference.

2.1 Interpolation methods for regular subdivisions

For a regular patch subdivision the sample points lie on a regular grid. Two well-known interpolation methods were used for this case, namely bilinear and bicubic spline interpolation.

The data for the following grid interpolation methods was the radiosity solution for a 16 by 16 regular subdivision of the ground patch. The first row of Fig. 3 shows this radiosity solution.

2.1.1 Bilinear interpolation

Bilinear interpolation is a linear interpolation in two directions. As we interpolate across a twodimensional patch, we determine the desired function value from the neighbours of the data point $\mathbf{q}$. We first have to determine the cell of the grid in which the desired data point falls. After that the function value for the data point is interpolated from the four vertices of the cell.

Let $(x_1, y_1), \ldots, (x_4, y_4)$ be the neighbours of $\mathbf{q} = (x_d, y_d)$, then $\tilde{B}(\mathbf{q})$ is determined as follows:

$$\begin{aligned} u &= (x_d - x_1)/(x_2 - x_1) \\ v &= (y_d - y_1)/(y_2 - y_1) \end{aligned}$$

$$\begin{aligned} \tilde{B}(x_d, y_d) = {} & (1-u)(1-v)B(x_1, y_1) + \\ & u(1-v)B(x_2, y_2) + \\ & u\, v\, B(x_3, y_3) + (1-u)v\, B(x_4, y_4) \end{aligned}$$

The second row of Fig. 3 shows the application of bilinear interpolation. The most noticeable artefact is a light leak under the wall, also to be seen in the difference image. That is a well-known problem when using this type of interpolation for radiosity reconstruction. Another problem with this interpolation method is that the result has a discontinuous first derivation across cell boundaries, sometimes visible as Mach bands.

2.1.2 Bicubic spline interpolation

To avoid discontinuities across cell boundaries one can switch to higher order interpolation eg bicubic spline interpolation. We use natural cubic splines that have a zero second derivative at the boundary. To determine a value for a data point (x_d, y_d) in a $m \times n$ grid we first evaluate m one dimensional splines for y_d. After that we evaluate the one dimensional spline from this values and x_d to retrieve the function value $\tilde{B}(x_d, y_d)$. Further details can be found in [PTVF92].

The solution resulting from this interpolation method can be seen in the third row of Fig. 3. The higher continuity of bicubic spline interpolation avoids Mach bands but an even more distractable artefact is introduced by oscillations of the interpolation, visible as alternating dark and bright stripes parallel to the shadow edge.

2.2 Interpolation methods for adaptive subdivisions

Adaptive subdivision of patches for radiosity calculations was introduced by Cohen et al. [CGIB86] and generalized to the notion of hierarchical radiosity by Hanrahan et al. [HSA91]. Common to these approaches is the hierarchical, quadtree-like subdivision of the patches (cf. Fig. 1).

Using scattered data interpolation, one tries to reconstruct a function from arbitrary located sample points. The samples need not be aligned on a grid. For the use of scattered data interpolation in general and especially in the field of geometric deformations compare [Rup94, RM93].

The data for the following scattered data interpolation methods was the radiosity solution for an adaptive quadtree subdivision of the ground patch, that resulted in 286 subpatches. The first row of Fig. 4 shows this radiosity solution.

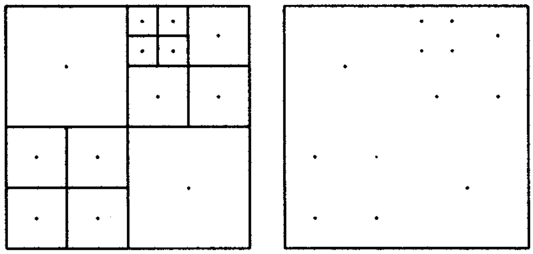

Figure 1: Quadtree subdivision and sample points

We present three scattered data interpolation methods which we have implemented to see their impacts on visualisation of radiosity functions across scene patches.

2.2.1 Distance weighted interpolation

One of the simplest methods for scattered data interpolation is distance weighted interpolation or Shepard's method [She68]. Every sample point has influence on the function value for a data point. The influence of a sample point $\mathbf{p}_i$ depends on its distance to the desired data point $\mathbf{q}$.

$$\tilde{B}(\mathbf{q}) = \sum_{i=1}^{n} w_i(\mathbf{q})\ B(\mathbf{p}_i)$$

The w_i are weights which are dependent from the distance between the desired data point $\mathbf{q}$ and the sample points $\mathbf{p}_i$. The w_i have to fulfill the conditions

$$\begin{aligned} w_i(\mathbf{p}_i) &= 1, \\ \sum_{i=1}^{n} w_i(\mathbf{q}) &= 1, \\ w_i(\mathbf{q}) &\geq 0. \end{aligned}$$

Shepard chose

$$\begin{aligned} w_i(\mathbf{q}) &= \frac{\sigma_i(\mathbf{q})}{\sum_{i=1}^{n} \sigma_i(\mathbf{q})} \\ \sigma_i(\mathbf{q}) &= \frac{1}{d(\mathbf{q}, \mathbf{p}_i)^{\mu}} \end{aligned}$$

resulting in:

$$\tilde{B}(\mathbf{q}) = \frac{\sum_{i=1}^{n} d(\mathbf{q},\mathbf{p}_i)^{-\mu} B(\mathbf{p}_i)}{\sum_{i=1}^{n} d(\mathbf{q},\mathbf{p}_i)^{-\mu}}$$

Distance weighted interpolation was applied to the quadtree data (second row of Fig. 4). From the images one can see that distance weighted interpolation has the drawback that it tends to produce poles around the sample values. Because of this disadvantage other methods were implemented and tested.

2.2.2 Hardy's Multiquadrics

An interpolation scheme that does not produce the undesired poles is Hardy's Multiquadrics. The basic idea is to describe the interpolating function as a linear combination of basis functions f_i and to determine the coefficients α_i of the base functions. Normally, base functions which depend only on the distance to a sample point $\mathbf{p}_i$ are used. They are called radial basis functions. Our interpolating function becomes:

$$\tilde{B}(\mathbf{q}) = \sum_{i=1}^{n} \alpha_i \; f_i(d(\mathbf{q},\mathbf{p}_i)) \qquad (1)$$

Hardy chose $f(d) = (d^2 + r^2)^{\mu}, r > 0, \mu \neq 0$. r can be choosen freely in general, but Eck [Eck91] proposes to associate an individual r_i with every sample point as $r_i = \min_{i \neq j} d(\mathbf{p}_i, \mathbf{p}_j)$. The α_i are determined by solving the linear equations resulting from solving equation (1) for the sample points and using the auxiliary conditions $\tilde{B}(\mathbf{p}_i) = B(\mathbf{p}_i)$. We use Gauss-Jordan elimination from [PTVF92] to solve the linear equations.

To achieve higher precision, one can add d-variate polynomes to the sum of equation (1). We have not used any additional polynomes.

The results of this method can be seen in the third row of Fig. 4 for the quadtree data. Similar to bicubic spline interpolation this method shows oscillations resulting from the linear combination of basis functions with positive and negative coefficients.

2.2.3 Natural neighbour interpolation

In subsection 2.2.1 we gave some conditions the weight functions have to obey to be suitable for the interpolation. As long as these conditions are fulfilled, any function is suitable as a weight function. Natural neighbour interpolation [Sib81] utilizes a function λ that has the following properties:

$$\lambda_i(\mathbf{q}) = \frac{v(\mathcal{VR}_i(\mathbf{q}))}{v(\mathcal{VR}(\mathbf{q}))}$$

v determines the area of a region. $\mathcal{VR}(\mathbf{q})$ is the Voronoi region of a point $\mathbf{q}$.

$$\mathcal{VR}(\mathbf{q}) = \{\mathbf{p} \in \mathbb{R}^2 | d(\mathbf{p},\mathbf{q}) \leq d(\mathbf{p},\mathbf{p}_j), \forall j = 1,\ldots,n\}.$$

$\mathcal{VR}_i(\mathbf{q})$ is the sub region $\mathcal{VR}(\mathbf{q}) \cap \mathcal{VR}_i$ where $\mathcal{VR}_i$ is the point set

$$\mathcal{VR}_i = \{\mathbf{p} \in \mathbb{R}^2 | d(\mathbf{p},\mathbf{p}_i) \leq d(\mathbf{p},\mathbf{p}_j), \forall j = 1,\ldots,n\}, \quad i = 1,\ldots,n.$$

Each $\lambda_i(\mathbf{q})$ represents one so called *natural neighbour coordinate.* With these coordinates we can set up our interpolating function $\tilde{B}(\mathbf{q})$.

$$\tilde{B}(\mathbf{q}) = \sum_i \lambda_i(\mathbf{q}) \; B(\mathbf{p}_i)$$

We used the program `nngridr`, an implementation of natural neighbour interpolation from Dave Watson [Wat94].

Images generated with natural neighbour interpolation can be found in the third row of Fig. 4. The difference image shows a small light leak along the wall. A slight problem occurs along the border of the ground patch where the method changes from interpolation to extrapolation. This can be fixed by adding additional sample points along the border, this will be the subject of further research.

2.3 Numerical errors

Tables 1 and 2 show the error measures of the difference images in different error norms known from approximation theory. The L^1 norm measures the mean error, L^2 ist the mean squared error and L^∞ is the maximum difference between the interpolation $\tilde{B}$ and the reference solution B. One thing to notice is that different error norms

interpolation method	L^1	L^2	L^∞
piecewise constant	0.00506	0.000226	0.337
bilinear	0.00746	0.000842	0.329
bicubic	0.0142	0.00107	0.31
distance weighted	0.00685	0.000487	0.333
Hardy	0.0113	0.00087	0.329
natural neighbour	0.0127	0.00135	0.329

Table 1: Errors for reconstruction of grid data

interpolation method	L^1	L^2	L^∞
piecewise constant	0.014	0.000622	0.169
distance weighted	0.0742	0.00964	0.302
Hardy	0.033	0.00244	0.412
natural neighbour	0.0328	0.00273	0.329

Table 2: Errors for reconstruction of quadtree data

result in different rankings, eg the bicubic interpolation has the biggest L^1 error but the smallest L^∞ error. The second thing we noticed is that this error measures applied to our scene are not suitable to compare (subjective) visual quality of the reconstructed images. The piecewise constant radiosity function, that is the originally calculated radiosity without interpolation, has in all cases but one the smallest error. It is obvious that no interpolation method improves the radiosity in a numerical sense.

3 Conclusion

We have shown and discussed the quality of several interpolation methods used to reconstruct radiosity from samples across patches. Special attention was given to scattered data interpolation methods which are widely accepted in other application areas.

While higher order interpolation produced visual artefacts resulting from oscillation of the interpolation function, scattered data interpolation, especially natural neighbour interpolation, has shown to achieve acceptable results.

It is difficult to propose a specific interpolation method because no interpolation method decreases L^1 or L^2 errors and while we think that natural neighbour interpolation is suitable to reconstruct the radiosity function, all visual quality enhancements are subjective.

The use of scattered data interpolation for radiosity reconstruction is technically independent from the meshing used to generate radiosity samples. This makes it easy to swap to this kind of interpolation in order to increase visual quality when advanced meshing algorithms like discontinuity meshing are not available.

Although bilinear interpolation is implemented in hardware in some graphics workstations, it has the disadvantage that it cannot be used directly when radiosity is calculated only at scattered locations across the patch. Additional triangulation or restricted quadtrees have to be used. Scattered data interpolation can be directly applied to the sampled radiosity values.

References

[Alf89] P. Alfeld. Scattered data interpolation in three or more variables. In T. Lyche and L. Schumaker, editors, *Mathematical Methods in Computer Aided Geometric Design*, pages 1–34. Academic Press, 1989.

[BdSF93] Rui Manuel Bastos, António Augusto de Sousa, and Fernando Nunes Ferreira. Reconstruction of Illumination

Functions using Bicubic Hermite Interpolation. In *Proceedings of Fourth Eurographics Workshop on Rendering*, pages 317–326, 1993.

[BGZ96] Rui Bastos, Michael Goslin, and Hansong Zhang. Efficient Rendering of Radiosity Using Textures and Bicubic Reconstruction. Technical report, Dept. of CS, U. of North Carolina at Chapel Hill, 1996. TR 96-025.

[CGIB86] Michael F. Cohen, Donald P. Greenberg, David S. Immel, and Philip J. Brock. An efficient radiosity approach for realistic image synthesis. *IEEE Computer Graphics and Applications*, 6(3):26–35, March 1986.

[CW93] Michael F. Cohen and John R. Wallace. *Radiosity and Realistic Image Synthesis*. Academic Press Professional, Boston, MA, 1993.

[Eck91] M. Eck. Interpolationsmethoden zur Rekonstruktion von 3D-Oberflächen aus ebenen Schnittfolgen. *CAD und Computergraphik*, 13(5):109–120, February 1991.

[GTGB84] Cindy M. Goral, Kenneth K. Torrance, Donald P. Greenberg, and Bennett Battaile. Modelling the interaction of light between diffuse surfaces. *Computer Graphics*, 18(3):213–222, July 1984.

[HSA91] Pat Hanrahan, David Salzman, and Larry Aupperle. A rapid hierarchical radiosity algorithm. *Computer Graphics*, 25(4):197–206, July 1991.

[LTG92] Dani Lischinski, Filippo Tampieri, and Donald P. Greenberg. Discontinuity meshing for accurate radiosity. *IEEE Computer Graphics and Applications*, 12(6):25–39, November 1992.

[Nie93] Gregory M. Nielson. Scattered data modeling. *IEEE Computer Graphics and Applications*, 13(1):60–70, January 1993.

[PTVF92] William H. Press, Saul A. Teukolsky, William T. Vetterling, and Brian P. Flannery. *Numerical Recipes in C.* Cambridge University Press, second edition edition, 1992.

[RM93] Detlef Ruprecht and Heinrich Müller. Free form deformation with scattered data interpolation methods. In G. Farin, H. Hagen, and H. Noltemeier, editors, *Geometric Modelling (Computing Suppl. 8)*, pages 267–281. Springer Verlag, Wien, 1993.

[Rup94] Detlef Ruprecht. *Geometrische Deformationen als Werkzeug in der grafischen Datenverarbeitung.* PhD thesis, University of Dortmund, 1994. published by Verlag Shaker, 1995, ISBN 3-8265-0451-8.

[She68] D. Shepard. A two-dimensional interpolation function for irregularly-spaced data. In *Proceedings of the ACM national conference*, pages 517–524, 1968.

[Sib81] R. Sibson. A brief description of natural neighbour interpolation. In Vic Barnett, editor, *Interpreting Multivariate Data*, pages 21–36. Wiley, New York, 1981.

[SLD92] David Salesin, Daniel Lischinski, and Tony DeRose. Reconstructing Illumination Functions with Selected Discontinuities. In *Third Eurographics Workshop on Rendering*, pages 99–112, Bristol, UK, May 1992.

[Wat94] Dave Watson. `nngridr`, *An Implementation of Natural Neighbour Interpolation.* David F. Watson, P.O. Box 734, Claremont, WA 6010, Australia, 1994.

[Whi80] Turner Whitted. An improved illumination model for shaded display. *Communications of the ACM*, 23(6):343–349, 1980.

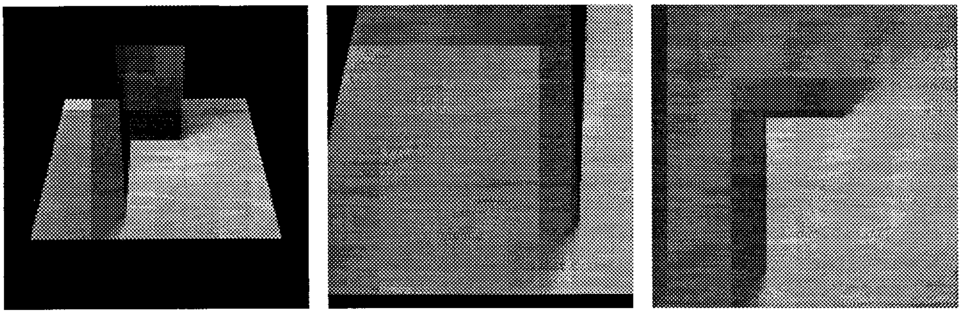

Figure 2: Reference solution with regular grid, 400 by 400

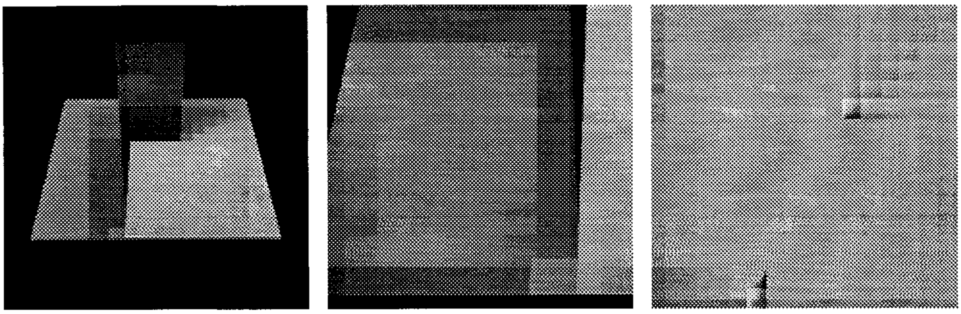

radiosity solution (piecewise constant)

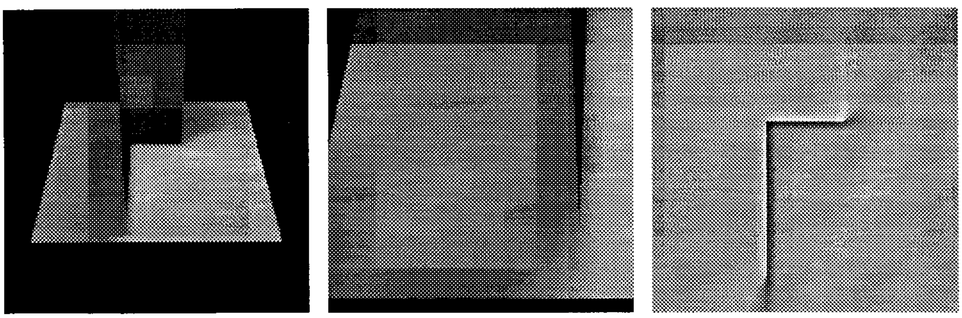

bilinear interpolation

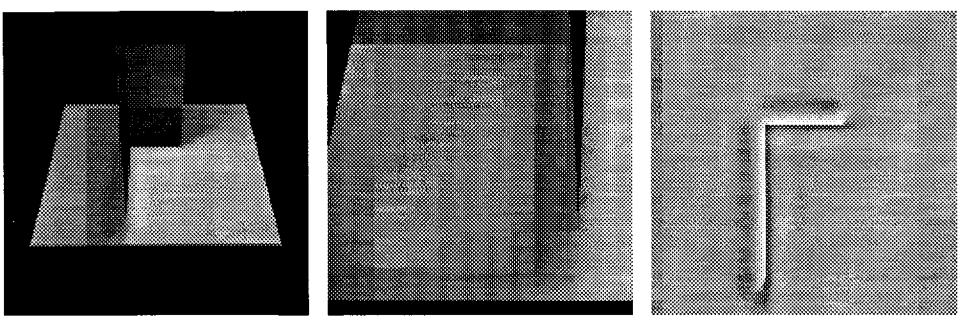

bicubic spline interpolation

Figure 3: Radiosity solution with regular grid, 16 by 16

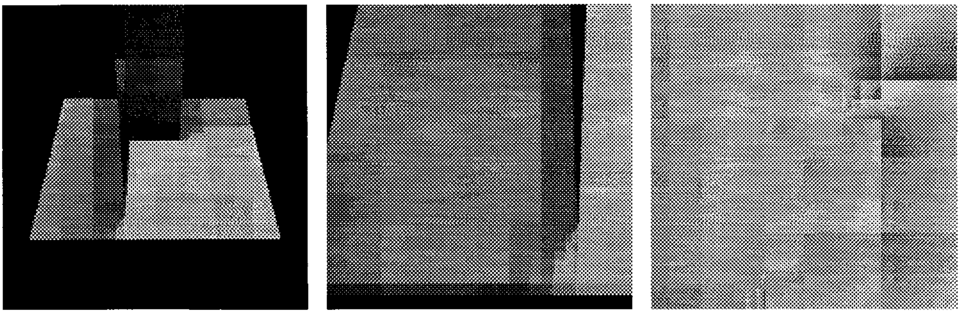

radiosity solution (piecewise constant)

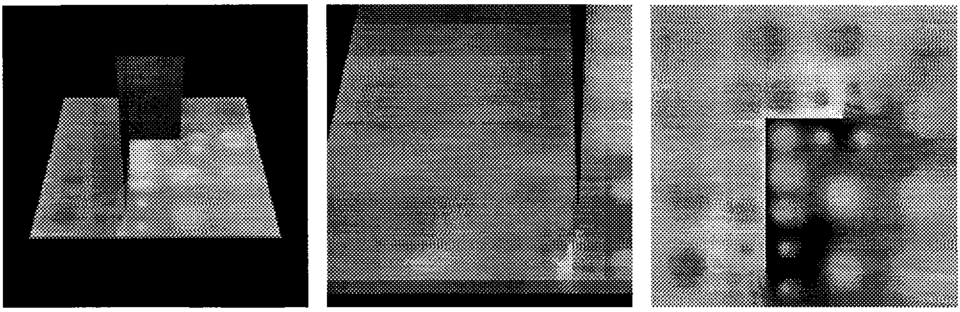

distance weighted interpolation, $\mu = 4$

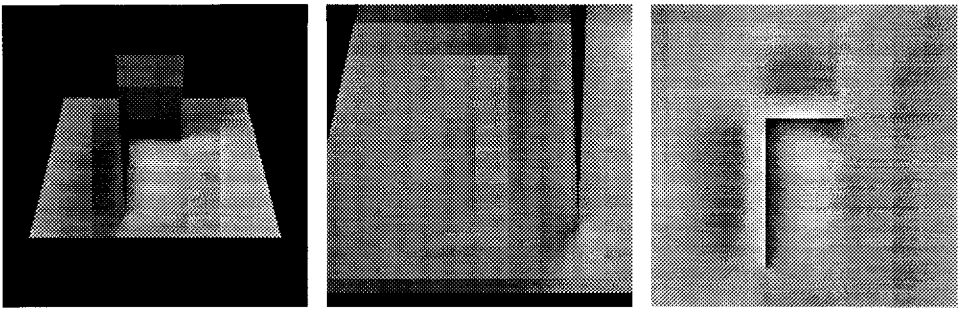

Hardy's multiquadric

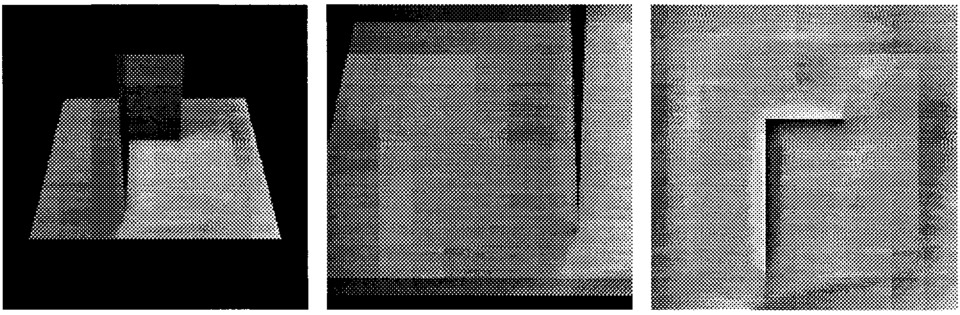

natural neighbour interpolation

Figure 4: Radiosity solution with quadtree subdivision